J Mater Sci

Energy materials

The promise of solution-processed Fe_2GeS_4 thin films in iron chalcogenide photovoltaics

Mimi Liu[1], Dominik M. Berg[1,2], Po-Yu Hwang[1], Cheng-Yu Lai[1], Kevin H. Stone[3], Finn Babbe[4], Kevin D. Dobson[5], and Daniela R. Radu[1,6,*]

[1] *Department of Chemistry, Delaware State University, Dover, DE 19901, USA*
[2] *Department of Physics and Astronomy, Rowan University, Glassboro, NJ 08028, USA*
[3] *SLAC National Accelerator Laboratory, 2575 Sand Hill Road, Menlo Park, CA 94025, USA*
[4] *Physics and Materials Science Research Unit, University of Luxembourg, 4422 Belvaux, Luxembourg*
[5] *Institute of Energy Conversion, University of Delaware, Newark, DE 19716, USA*
[6] *Department of Materials Science and Engineering, University of Delaware, Newark, DE 19716, USA*

Received: 10 October 2017
Accepted: 27 January 2018

ABSTRACT

The olivine Fe_2GeS_4, featuring non-toxic elements, cost-effective synthesis, and suitable optoelectronic properties, recently emerged as a promising light-absorbing candidate. Fe_2GeS_4 precursor powders obtained via a simple solution-based process were converted to highly crystalline Fe_2GeS_4 powders upon a thermal treatment in controlled atmosphere. Thin films fabricated by dip coating in the Fe_2GeS_4 precursor dispersion and subjected to the same thermal treatment render high-purity Fe_2GeS_4 thin films with a band gap of 1.4 eV, measured by room-temperature photoluminescence. Using Fe_2GeS_4 thin films as the sole absorber in a solution-based solar cell, open-circuit voltages of 361 mV are observed, while the use of the Fe_2GeS_4 films as counter electrodes in dye-sensitized solar cell constructs enhances the overall power conversion efficiency of the cell by a factor of five. This is the first report of a photovoltaic device based on Fe_2GeS_4.

Introduction

Solar energy is considered a promising alternative to fossil fuels for its excellent advantages as an abundant, renewable, and clean source of energy. The first silicon solar cell was reported by Russell in 1941 [1], and ever since, silicon solar cells were developed, commercialized, and currently account for more than 90% of solar market. Given the high cost to produce silicon-type solar cells in the past, solar research advanced to the second generation of constructs, comprising thin-film approaches, toward lowering the overall solar cell cost through inexpensive materials and fabrication technologies [2].

Thin-film amorphous silicon, $Cu_2(In,Ga)Se_2$ (CIGS), and CdTe, the three major Gen II solar cells, have been successfully developed and

Address correspondence to E-mail: dradur@desu.edu

https://doi.org/10.1007/s10853-018-2082-1

Published online: 06 February 2018

commercialized [3]. Despite their overall success of reaching power conversion efficiencies of up to 22.6% [4], CIGS and CdTe solar cells are plagued by the supply limitations and increasing price of rare elements such as indium (In) and gallium (Ga) [5]. Besides, both technologies require the use of toxic elements such as selenium (Se) and cadmium (Cd) baring health risks for researchers and manufacturers [6]. Therefore, the demand of alternative, Earth-abundant, non-toxic elements drove the quest for novel absorber materials.

In 1986, pyrite (FeS_2) was viewed as a good alternative to CIGS and CdTe due to its low toxicity and elements abundance, while offering a large absorption coefficient ($> 10^5$ cm^{-1}) and a band gap suitable for photovoltaic (PV) applications ($\sim$ 0.95 eV) [7]. Unfortunately, until today pyrite-based devices display low power conversion efficiencies of 7% [8], which does not match the theoretical efficiency of 20% and cannot compete with CIGS or CdTe technologies [9]. FeS_2-based solar cell has been impaired by thermal instability [10], phase coexistence [11], and performance problems [7]. Yu et al. pointed to an intrinsic thermal instability of the FeS_2, along with other considerable challenges that must be overcome for obtaining high-quality, single-phase FeS_2 films; the study concluded that for effective solar absorption and henceforth a ligand field splitting of sufficient magnitude for the Fe^{2+}, the Fe^{2+} ion must be bound by at least six sulfur atoms, requiring the Fe^{2+} cation in an octahedral site. The group predicted that the addition of a third element with an electronegativity favoring strong covalent bonding with sulfur would further stabilize the octahedral site Fe^{2+}. Ge and Si have been demonstrated to fulfill the stabilization requirements, rendering Fe_2SiS_4 and Fe_2GeS_4 compounds which do not readily decompose into S-deficient binary phases. Noteworthy, both materials inherited pyrites superb optoelectronic properties with nearly ideal band gaps (Fe_2SiS_4—calculated: 1.55 eV, measured: 1.54 eV; and Fe_2GeS_4—calculated: 1.40 eV, measured: 1.36 eV) and similar absorption coefficients ($> 10^5$ cm^{-1}) [10]. This suggested the opportunity to work with ultra-thin films, smaller than 1 μm in thickness, along with all the related advantages, including lower materials consumption, homogeneity and impurity control (compared with thicker films), and potential use of flexible substrates.

Fe_2SiS_4 was shown to be very sensitive to air and moisture, while its germanium counterpart, Fe_2GeS_4, (FGS) has a much higher stability in air, hence making it a better candidate in developing iron chalcogenide PV absorbers [12].

In addition to the quest for novel thin-film materials, solution-processed absorbers have attracted a lot of attention which impacted the new-coming FGS; since Yu et al.'s seminal article [10], predicting FGS potency as a PV absorber, all current reports of FGS materials refer to nanoparticle preparations toward solution processable routes.

Two major synthetic routes for fabricating FGS nanomaterials have been reported: solvothermal [13, 14] and mechanochemical [15]. Prieto's group synthesized FGS nanoparticles through a 24-h reaction, a fairly long and energy-intensive process. No PV device has been reported; however, the FGS nanoparticles, cast in a thin film, showed a small photocurrent measured by a photo-electrochemical setup [13]. Lim's group synthesized FGS nanosheets through an alternative solvothermal route, requiring a two-step and 5.5-h process; the report did not include a PV device. However, the nanosheets exhibited a measured band gap of 1.38 eV [14].

In the mechanochemical approach, Park's group synthesized Fe_2GeS_4 nanocrystals in a 12-h process. The report included Raman scattering experiments revealing a FGS-related peak at 361 cm^{-1}. The post-synthetic annealing of the mechanochemically obtained material rendered FGS with a 1.43 eV band gap [15].

We are reporting herein a facile synthetic method for a FGS precursor powder that, upon annealing in sulfur and argon atmosphere, renders pure FGS. The synthesis of precursor powder was highly optimized to produce a stable product. Inks fabricated from the FGS precursor powders were annealed to render highly crystalline FGS thin films.

The successful fabrication of highly crystalline FGS thin films enabled us to construct the first thin-film FGS functional solar device fabricated with a solution-based photovoltaic cell. The modest efficiency of the device 0.03% could be attributed to the overall short-circuit current density (J_{sc}) of 0.19 mA/cm^2, while the respectable open-circuit voltage of 361 mV for this first FGS-based device indicates the potential of FGS as a photovoltaic absorber.

Materials and methods

Materials

Glycolic acid (99%), diethyl ether (99%), and oleylamine (OLA) (70%) were purchased from Sigma-Aldrich. GeO_2 (99.99%) was purchased from MSE Supplies. Fe(III) 2,4-pentanedionate, sulfur (99.5%), and 1-octadecene (ODE) (90%) were purchased from Alfa Aesar. ACS grade acetone (99.8%), chloroform (99.8%), ethanol (99.5%), toluene (99.7%), and methanol (99.8%) were purchased from VWR International. Sputtered 0.7-μm molybdenum-coated soda-lime grass (Mo-SLG) substrates were obtained from the Institute of Energy Conversion, University of Delaware. Glass substrates were purchased from Fisher Scientific. Indium tin-oxide (In–SnO_2 or ITO)-coated glass substrates, 3–5 Ω/sq, were purchased from MSE Supplies. TiO_2 paste, iodide/tri-iodide electrolyte, and (*cis*-diisothiocyanato-bis (2,2′-bipyridyl-4,4′-dicarboxylato) ruthenium(II) bis (tetrabutylammonium), dye or "*ruthenizer 535-bis TBA*" were purchased from Solaronix. All chemical reagents and solvents were used as received and without further purification.

Synthesis of diaquabis (glycolato-O,O′′) germanium(IV)—$Ge(Gly)_2(H_2O)_2$

The compound was synthesized through a modified published procedure by Chiang et al. [19]. In a typical experiment, germanium dioxide (GeO_2) (0.52 g, 5.0 mmol) was added to a 100 mL pre-prepared aqueous solution of glycolic acid (1.52 g, 20.0 mmol). The reaction mixture was further refluxed for 4 h. Upon cooling, the final solution was reduced to ~ 5 mL via rotary evaporation. The $Ge(Gly)_2(H_2O)_2$ powder was precipitated by adding a 1:1 Et_2O:EtOH and collected by filtration. $Ge(Gly)_2(H_2O)_2$ was store under vacuum.

Synthesis of Fe_2GeS_4 precursor powder with OLA–ODE solvent mixture

In a typical experiment, $Ge(Gly)_2(H_2O)_2$, (0.957 g, 3.73 mmol), 10 mL degassed OLA, and 5 mL ODE were added to a 100-mL two-neck round-bottom quartz flask. Separately, Fe(III) 2,4-pentanedionate (2.119 g, 6 mmol) was dissolved in a mixture of 10 mL degassed OLA and 5 mL ODE in a two-neck round-bottom glass flask. Sulfur powder (0.384 g, 12 mmol) was dissolved in a mixture of 10 mL degassed OLA and 5 mL ODE in a two-neck round-bottom glass flask. Each of the three solutions was stirred at 120 °C for 30 min under vacuum to remove moisture. The formed Fe(III) solution was then injected into the Ge(IV) solution at 120 °C, and the reaction mixture was held at the same temperature for 10 min, followed by heating to 250 °C. Meanwhile, the sulfur solution was heated and held at 150 °C. When both solutions reached the target temperatures, the sulfur solution was added dropwise to the Fe–Ge solution. The final solution was held at 250 °C for 15 min, the actual reaction time. Afterward, the reaction was cooled to room temperature by removing the heating source and the product was purified with a 1:2 $CHCl_3$:ethanol solvent mixture. The resulting solid product was dried under vacuum.

Synthesis of Fe_2GeS_4 precursor powder using OLA as solvent

Synthesis of Fe_2GeS_4 precursor powder using OLA followed the same route to the above synthesis but using only OLA (in the indicated amounts) as solvent.

Fe_2GeS_4 annealing

For studying the ability of precursor powder to generate high-purity FGS, the precursor powders were subjected to a thermal treatment under a sulfur and argon atmosphere in a tube furnace at 550 °C.

Preparation of Fe_2GeS_4 precursor inks

In a typical experiment, 300 mg of FGS precursor powder was suspended in a mixture of 1.5 mL ethanol and 12 mL toluene and sonicated for 6 min with an ultrasonic probe. The resulting dispersions (inks) were immediately used for films fabrication without further storage.

Fabrication of Fe_2GeS_4 thin films

All films were deposited on either soda-lime glass or Mo-coated soda-lime glass substrates. The substrates were cleaned in an ultrasonic bath using sequentially: methanol, nanopure water, and acetone. Finally, the

substrates were dried and subjected to plasma cleaning.

Upon cleaning, each substrate was dip-coated in the FGS precursor ink. Each substrate was manually immersed into the Fe_2GeS_4 precursor inks slowly, followed by 3 s of immersion time; next, the substrate was pulled upward slowly. Subsequently, the as-deposited thin film was air-dried. The entire dip-coating process was repeated for nine consecutive times. This number was chosen by an SEM cross-section analysis of post-annealed films (see also figure S1).

Upon completing the 9-layer deposition, each film was further subjected to thermal treatment under a sulfur and argon atmosphere in a tube furnace for a combination of times and temperatures, ranging from 1 to 3 h and 400–600 °C, respectively, toward optimizing film purity and stability. The sulfur atmosphere was supplied through slow evaporation of sulfur powder, introduced simultaneously with the samples in a crucible placed in the ~ 350 °C zone of the tube furnace.

Solar cells fabrication

The thermally treated films were processed into solar cells. A Fe_2GeS_4-catalyzed dye-sensitized solar cell (DSSC) was fabricated following a procedure adapted from Xin et al. [17]. For the present study, TiO_2 films were bar-coated onto fluorine-doped tin-oxide (FTO) substrates and subsequently fast-dried at 300 °C for 5 min on a hot plate, in air, in order to remove the organic solvent. Afterward, the TiO_2 films were soaked overnight in a methanolic solution of ruthenizer 535-bis TBA (0.3 mmol/L), following a procedure reported by Grätzel's group [20]. The dye-stained TiO_2 film was further rinsed with methanol and assembled face-on to the Fe_2GeS_4/Mo thin film in a sandwich form. Two drops (100 µL) of iodide/tri-iodide electrolyte were then added into the gap between the two electrodes. The final device had a layered structure as follows: ITO/TiO_2&Dye/Iodine solution/FGS/Mo. In a control experiment aiming to separate the contribution of the FGS from the dye, a Fe_2GeS_4-solution-based solar cell was fabricated. All aforementioned fabrication steps have been repeated excepting the addition of the dye to the TiO_2 films, resulting in a final device structure as follows: ITO/TiO_2/iodine solution/FGS/Mo. Lastly, a control DSSC device made without FGS was also fabricated, with the structure: ITO/TiO_2&Dye/Iodine solution/Mo.

Characterization

X-ray diffraction (XRD) was performed on a Rigaku MiniFlex600 system equipped with a CuKα radiation source ($\lambda = 1.5405$ Å) and operated at 30 mV and 10 mA. Raman spectroscopy analysis was carried out on Horiba Scientific XploRA PLUS equipped with an Ar-laser source ($\lambda = 532$ nm). Elemental composition of the dried FGS powder was obtained by X-ray fluorescence (XRF) using a Rigaku Supermini200. Room-temperature photoluminescence (PL) spectra were recorded under continuous monochromatic illumination of an argon ion laser (514.5 nm). The PL was collected by two off-axis mirrors, spectrally resolved by a grating monochromator and detected by a Si-CCD array. The current–voltage dependence of the solar cell devices was recorded using a Keithley 2400 source meter under simulated solar light generated by the Small Area Solar Simulator from Newport (LCS-100TM) operating at 1.0-sun output using a 100-W xenon lamp with integrated reflector (1000 W/m^2 at 25 °C and AM1.5G). All devices were measured in a top-down arrangement, while the light entered the solar devices through the ITO/TiO_2 side which was facing upwards.

Results and discussion

Preparation of the Fe_2GeS_4 precursor

Generation 2 (Gen 2) thin-film solar cells fabricated through solution methods require an annealing step upon absorber deposition, targeting high-quality, large-grain crystalline absorber layers. Therefore, the crystallinity of precursor materials prior to film deposition is not necessarily required. Both solvothermal and mechanochemical synthetic methods reported to date for producing FGS nanoparticle precursors are time-consuming, cumbersome, and energy-intensive processes [13–15] and therefore not economically feasible for absorber fabrication. In addition, the absence of a FGS solar device suggests the difficulty to provide robust absorber layers from any nanoparticles reported to date.

Interested in producing crystalline FGS films and PV devices, we have developed a solvothermal

method with a fast reaction time, which, after extensive optimization, rendered a precursor powder amenable to produce high-purity FGS upon thermal treatment in a sulfur and argon atmosphere.

Optimization of synthetic parameters involved Ge (IV) reagents as well as the solvent system used in the reaction.

In all FGS precursor powder syntheses, elemental sulfur was used as sulfur source and Fe(III) 2,4-pentanedionate ($Fe(acac)_3$) as Fe(III) source. Two Ge(IV) reagents have been tested: the commercially available GeI_4, and the in-house synthesized germanium glycolate, $Ge(Gly)_2(H_2O)_2$. Interestingly, when the synthesis of FGS precursor powder involved GeI_4 as the germanium source, only pyrrhotite was formed, upon powder annealing, as analyzed by XRD, regardless of the solvent system employed.

The use of $Ge(Gly)_2(H_2O)_2$ in the OLA-based synthesis of FGS precursor powder enabled, for the first time, to obtain high-purity, crystalline powders upon annealing at 550 °C in a sulfur/argon atmosphere as confirmed by synchrotron XRD (see also Figure S2). However, as illustrated in Fig. 1, if not annealed within 12 h after synthesis, the powder showed a fast color change (in less than 2 days). Upon annealing at 550 °C in sulfur/argon atmosphere, the aged powder made from a pure oleylamine (OLA) solvent synthesis formed pure pyrrhotite ($Fe_{0.789}S$).

Given the practical importance of improving precursor powder shelf life, various factors have been taken into consideration, including solvents used in the synthesis. Kauzlarich's group reported that Ge nanoparticles synthesized using alkenes, in particular octadecene (ODE), show high stability and resistance to oxidation [16]. Therefore, provided that such precautions might be related to the stability of the Ge precursor in the synthesis, we introduced ODE in our precursor powder syntheses as a co-solvent, and the product formed showed tremendous stability improvement, as indicated in Fig. 1. Comparing the XRD patterns of annealed products from both powders aged for 2 days (Fig. 1b) it is apparent that the annealed powder obtained from the OLA–ODE route forms a Fe_2GeS_4 phase.

X-ray fluorescence (XRF) composition measurements of the synthesized powder from the pure OLA solution revealed the Fe/Ge atomic percent ratio to be 2.3, while the mixed OLA and ODE solution had a Fe/Ge atomic percent ratio of 2.5. In both cases, the S/(Fe + Ge) ratio was around 1.2, indicating that the overall composition was close to stoichiometry.

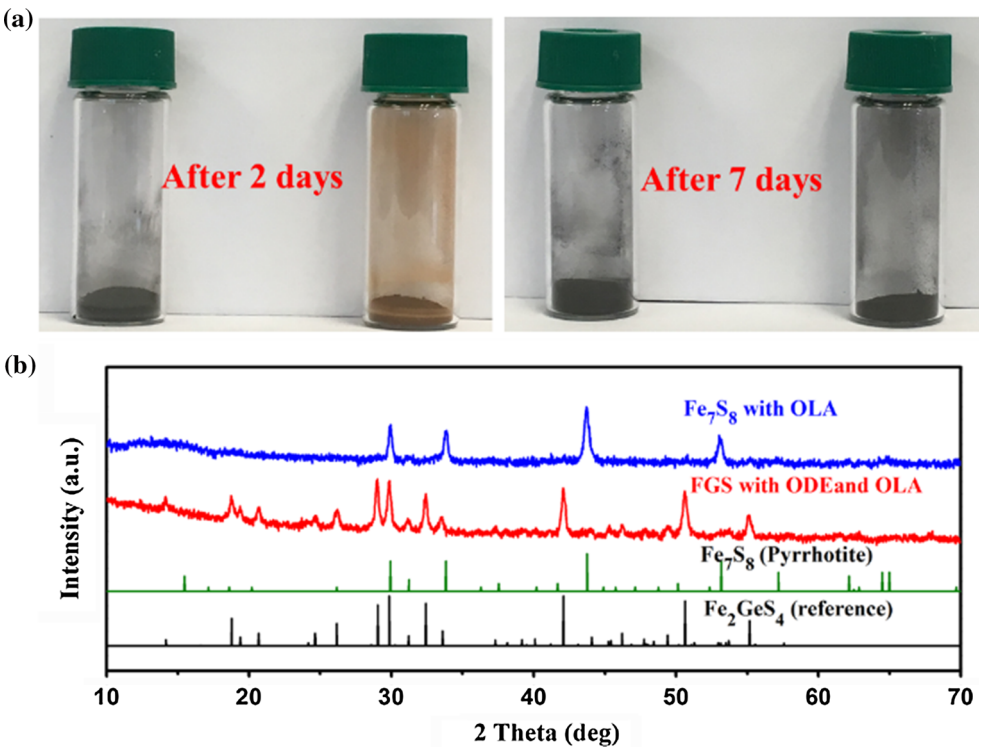

Figure 1 Stability of precursor powder. As-synthesized powders were stored for 48 h in ambient conditions and further annealed at 550 °C for 2 h in a sulfur and argon atmosphere. **a** Powder made using OLA as solvent (left) and powder made using a mixture of OLA and ODE (right). **b** XRD patterns of the annealed OLA-synthesized (blue) and the OLA–ODE mixture synthesized powder (red).

Crystalline Fe_2GeS_4 thin films

Toward obtaining films with thickness ~ 1 μm that could be used in thin-film solar cell constructs, FGS thin films were fabricated by dip coating. The deposited thin films were subsequently annealed at different temperatures, in sulfur/argon atmosphere, for 2 h, and 550 °C has been consistently observed as producing high-purity FGS (Fig. 2a). Film thickness, in the proximity of 1.3 μm, was observed by cross-section SEM (see Supporting information).

To further understand the impact of annealing time on FGS crystallinity and stability, the films were treated for different times, at 550 °C. As depicted in Fig. 2b, comparing XRD patterns of separate films annealed for 1, 2, and 3 h, respectively, indicates that no secondary phases were formed when the precursor powders were annealed for 2 h.

Figure 2c depicts the Raman spectra obtained of the annealed Fe_2GeS_4 thin film at 550 °C for 2 h. A Raman peak at 355.5 cm^{-1}, belonging to the olivine structure of Fe_2GeS_4 phase, is observed. These results are in agreement with reported Raman characteristics of FGS [15].

To validate the band gap of the FGS materials, photoluminescence (PL) spectroscopy measurements were taken on the film annealed at 550 °C for 2 h. To remove possible effects of the glass substrate on the spectral results, the thin film was lifted off the substrate using a two-component epoxy resin with no luminescence in the spectral region of interest. Figure 3 shows the PL spectra obtained at room temperature after subtracting the background illumination. Despite the low PL yield, a distinct PL peak is observed centered around 1.4 eV, giving a slight indication that the band gap of our FGS thin film is close to the value of 1.4 eV. Even though we cannot exclude that such a low PL yield at room temperature might be related to trap/defect luminescence, we believe that the measured PL spectrum likely shows the band-to-band transition as its energetic position, and hence, the rough value for the band gap is in very good agreement with the reported band gap values of 1.43 and 1.38 eV (UV–Vis spectroscopy) by Park et al. [15] and Lim et al. [14], respectively, and predicted and measured (UV–Vis) by Yu et al. [10].

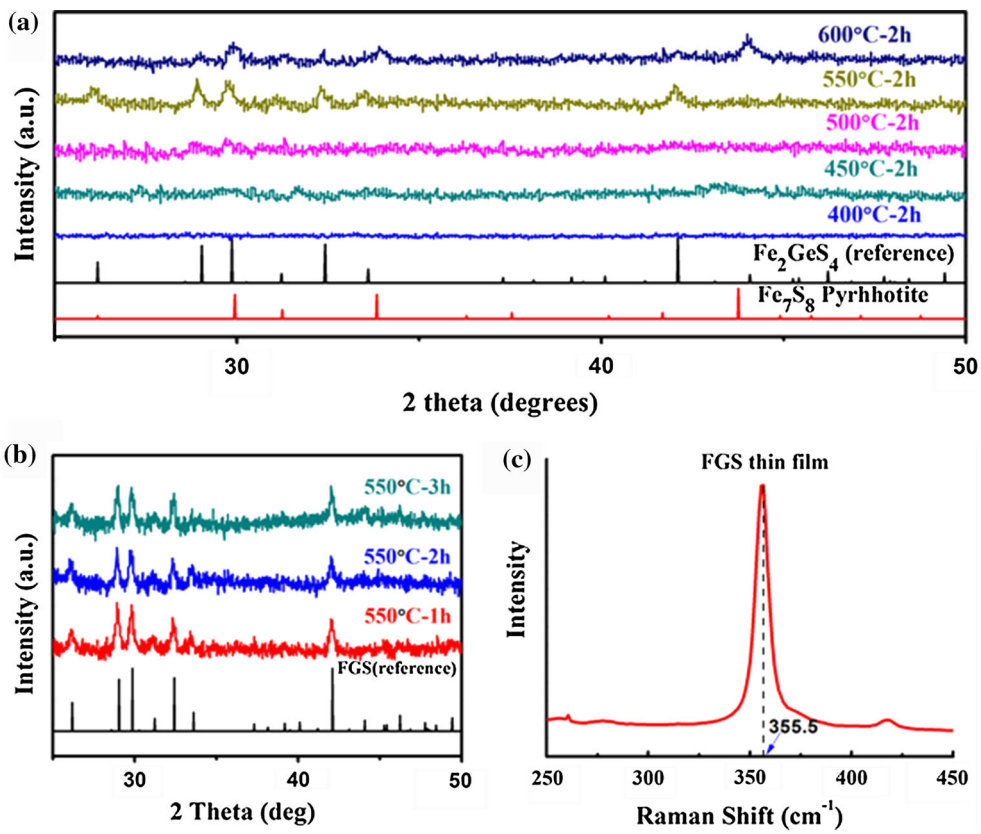

Figure 2 Optimization of Fe_2GeS_4 films processing. **a** Comparison of XRD patterns of FGS thin film annealed at different temperatures; **b** comparison of XRD patterns of FGS thin film annealed at 550 °C for different times. **c** Raman of FGS thin film annealed at 550 °C for 2 h.

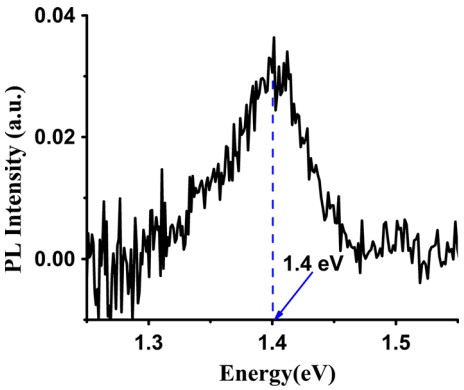

Figure 3 Fe_2GeS_4 thin-film band gap evaluation. Room-temperature PL spectrum of FGS crystalline thin film after subtracting the background.

Fe_2GeS_4 solar photovoltaic devices

Several recent publications have highlighted the potential of Fe_2GeS_4 as a candidate for photovoltaic devices [13–15], yet only one group has been able to measure a FGS-based photocurrent using a photoelectrochemical setup [13]. In the present study, we are showing the results for a FGS-catalyzed dye-sensitized solar cell and the results of the same construct in a control experiment where the dye is not included in the fabrication, toward decoupling the dye contribution from the FGS PV effect.

Xin et al. [17] suggested that chalcogenide semiconductors could replace platinum as efficient electrocatalyst counter electrodes in DSSC to improve solar cell efficiencies. In the study of Xin et al. and in subsequent studies such as that of Tong et al. [18], it was shown that chalcogenide semiconductors such as Cu_2ZnSnS_4 as a thin film on the counter electrode increase the overall solar cell efficiency by increasing the overall photocurrent. Following this approach, we have looked into the effects of a thin FGS layer on top of a Mo counter electrode on the overall power conversion efficiency. The overall fabrication flow, including precursor preparation and processing into the solar device, is depicted in Fig. 4.

Figure 5b shows the JV characteristics obtained from a standard dye-sensitized solar cell with the structure: ITO/TiO_2&Dye/Iodine solution/Mo. While the JV curve shows a significant open-circuit voltage (V_{OC}) of 467 mV, the short-circuit current density (J_{SC}) of 0.68 mA/cm^2 is fairly low. Introducing a thin film of FGS on the Mo substrate (changing the device structure to ITO/TiO_2&Dye/Iodine solution/FGS/Mo), the V_{OC} increased slightly to 544 mV while the short-circuit current increased significantly by a factor of six to 4.15 mA/cm^2, as depicted in Fig. 5a. This results in an overall power conversion efficiency increase from 0.14 to 0.71%. While we could only speculate on the decrease in fill factor for the added FGS layer at this point, the increase in J_{SC} due to the presence of a thin layer of FGS on the counter electrode could be originated in the added light absorption of the FGS thin films. At this moment, we would like to mention that we have repeated all presented experiments using fluorine-doped tin oxide (FTO) as a counter electrode, which is a commonly used counter electrode for DSSC. The overall results using FTO instead of Mo (not shown here) were slightly lower in device efficiencies but confirmed the overall trend that a FGS-coated back contact resulted in improved device efficiencies. This supports our hypothesis that the increase in J_{SC} due to the presence of a thin layer of FGS on the counter electrode could be originated in the added light absorption of the FGS thin films rather than an improved band alignment, which would be different for a Mo or an FTO back contact.

To decouple the light absorption in the FGS thin films from the light absorption in the dye, we have made a control FGS solution-based device without the addition of dye to the TiO_2 layer of the following structure: ITO/TiO_2/Iodine solution/FGS/Mo. In this device, the iodine solution is the electrical bridge between the *n*-type TiO_2 layer and the *p*-type FGS thin film where the majority of the light absorption is occurring. Figure 5c shows the JV characteristics in the dark and under illumination for such a solution-based photovoltaic device. Even though the overall short-circuit current density of 0.19 mA/cm^2 under illumination is very low, we measured a large open-circuit voltage of 361 mV resulting in a 0.03% efficient device. We attribute these low efficiencies to the very low J_{SC} as the measured open-circuit voltage of the device should be high enough to reach efficiencies in the single-digit range. Being able to obtain a high V_{OC} from a photoactive material is generally a key property for a photoactive material to be a good candidate for photovoltaic applications. A high V_{OC} means that the used absorbing material is capable of converting photonic energy into an energetic separation of electrons and holes in the conduction and valence bands, respectively. Measuring a V_{OC} of 361 mV for the FGS device, we can conclude that Fe_2GeS_4 is a potential

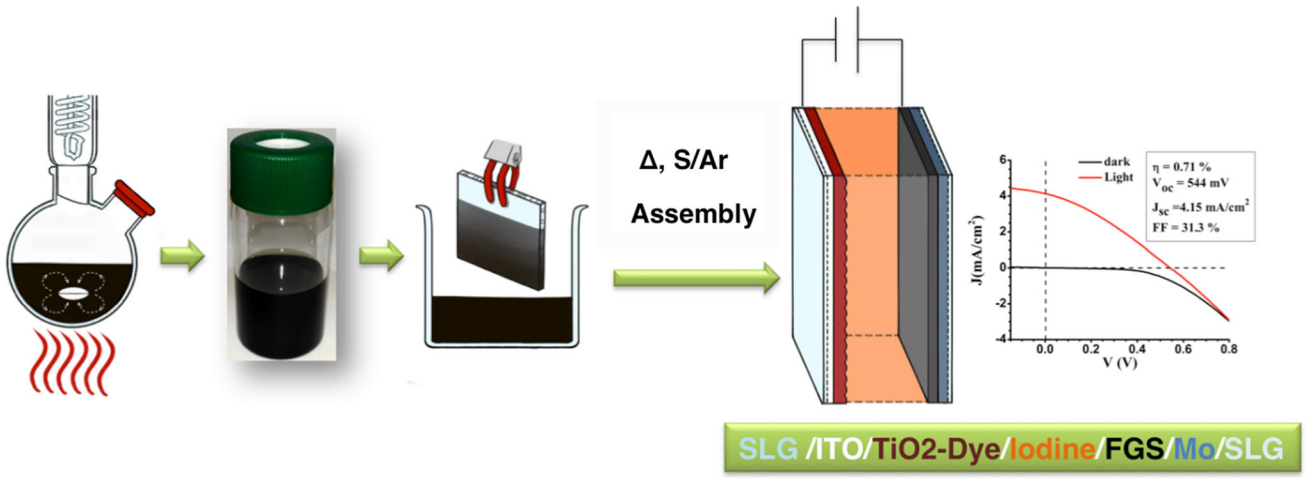

Figure 4 Fabrication process for Fe_2GeS_4-catalyzed dye-sensitized solar cell. The process encompasses Fe_2GeS_4 precursor synthesis and purification (step not shown); inks preparation (an actual Fe_2GeS_4 precursor ink is shown); molybdenum substrate coating with Fe_2GeS_4 ink via dip coating; solar device assembly in the DSSC architecture based on Fe_2GeS_4 film; and solar cell characteristics.

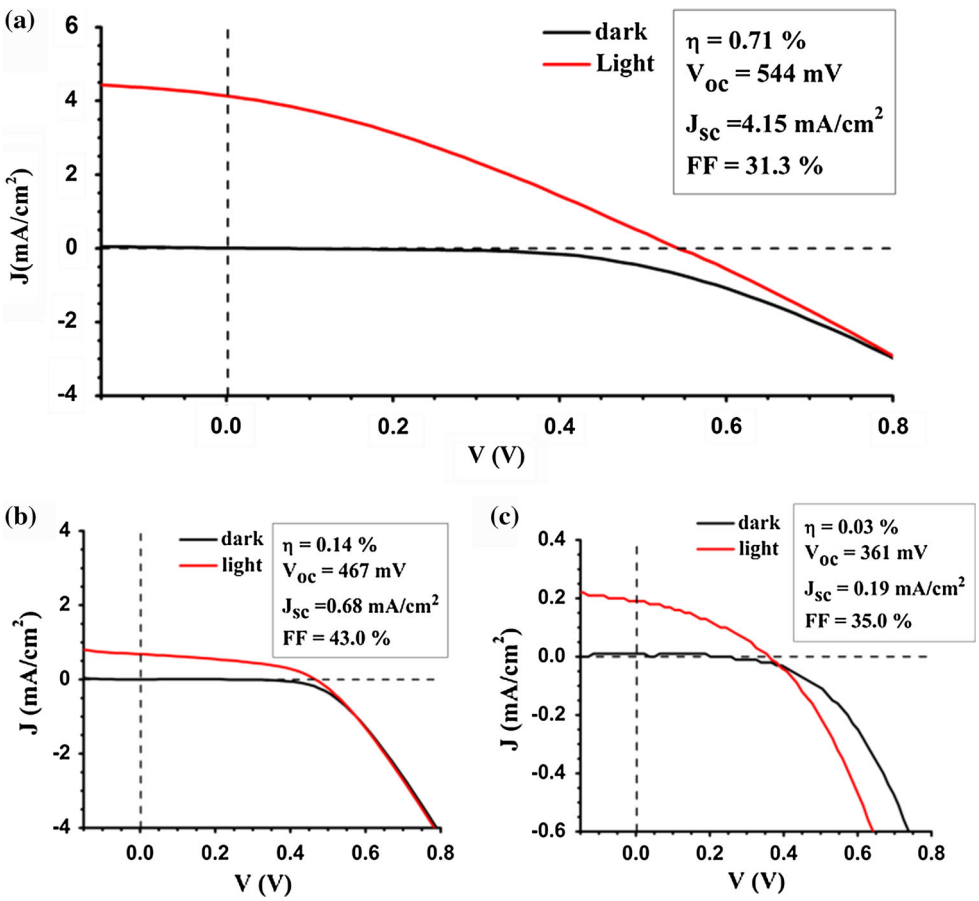

Figure 5 Device characteristics for Fe_2GeS_4 solar cell constructs. **a** Fe_2GeS_4-catalyzed dye-sensitized solar cell with Fe_2GeS_4 thin film; **b** control DSSC (same construct as without Fe_2GeS_4 thin film; **c** Fe_2GeS_4 solution-based solar cell: same construct as (**a**) without the dye.

candidate for photovoltaic applications. The low short-circuit current measured on our solution-based devices indicates that the presented solar cell device structure lacks the ability to extract this converted energy of the energetically separated electrons and holes into physically separating the charge carriers

from the absorbing region and driving a current. Speculating about the reason for a low current extraction, we could imagine that the presented devices could have a high density of defect states which would trap the charge carriers and lead to their recombination before they could be extracted. The SEM images shown in the supplemental information show a layered structure of small grains and hence a high density of grain boundaries. This could result in a high density of trap states which would limit the extraction of charge carriers and lead to a low J_{SC}, as observed. Attempts to measure external quantum efficiency on the samples were inconclusive. Further investigations in future studies are necessary to resolve the reason for the low photocurrent. The ineffectiveness of creating a photocurrent is generally not a good indicator of the potential performance of a photoactive material as such limitations can often be overcome by improving the thin-film quality or by enhancing and engineering a suitable device architecture around your photoactive material. From this, we conclude that—besides the low crystalline quality of the thin film and its potential connection to the low J_{SC}—the chosen device structure of the solution-based approach might not be the ideal structure for a solar cell based on Fe_2GeS_4. Hence, it is our main objective for future research on this material to move away from a solution-based device structure to a solid-state device structure in order to improve photocurrent through an improved charge carrier separation and with it the overall power conversion efficiency. The active area of all solar cell devices made in this work is 2.4 cm^2. The presented results for the open-circuit voltage of this first FGS-based solar cell reaffirm that Fe_2GeS_4 is a promising candidate for a low-cost material for photovoltaic applications and that higher efficiencies are possible with a more suitable solar cell structure.

Conclusions

We presented a solvothermal method that produces an amorphous precursor powder to Fe_2GeS_4. Synthesis optimization suggested that precursor powder stability is highly dependent of Ge(IV) source and the presence of octadecene in the reaction. Annealing of thin films fabricated from the precursor powder under a sulfur/argon atmosphere resulted in crystalline Fe_2GeS_4 thin film. Thermal treatment of 2 h at 550 °C was found optimal for obtaining high-purity Fe_2GeS_4 thin films. Room-temperature photoluminescence measurements of the annealed films showed low PL yield, however, sufficient to identify a band gap of roughly 1.4 eV for Fe_2GeS_4. When depositing as a thin layer on top of the counter electrode, Fe_2GeS_4 leads to an enhanced open-circuit voltage and power conversion efficiency. Furthermore, a solution-based solar cell with Fe_2GeS_4 as the absorber layer showed a significant open-circuit voltage of 361 mV highlighting the potentiality of FGS as a photoactive material.

Acknowledgements

This material is based upon work supported in part by the US Department of Energy SunShot Initiative (Award DE-EE0006322) and the National Science Foundation (Grants 1458980 and 1435716). Use of the Stanford Synchrotron Radiation Lightsource, SLAC National Accelerator Laboratory, was supported by the US Department of Energy, Office of Basic Energy Sciences under Contract No. DE-AC02-76SF00515. The authors would like to thank Dr. William Shafarman at the Institute of Energy Conversion at University of Delaware for valuable discussions regarding the solar cell results and to Dr. Susanne Siebentritt and Dr. Philip Dale for access to their research facilities.

Compliance with ethical standards

Conflict of interest The authors do not have competing interest and declare no conflict of interest.

Electronic supplementary material: The online version of this article (https://doi.org/10.1007/s10853-018-2082-1) contains supplementary material, which is available to authorized users.

References

[1] Ohl R (Original application May 27, 1941; published 1948, US2443542 A). Light-sensitive electric device including silicon. USPTO (ed). Bell Telephone Laboratories, Inc., Murray Hill

[2] Chopra KL, Das SR (1983) Why thin film solar cells? In: Chopra KL, Das SR (eds) Thin film solar cells. Springer, Boston, pp 1–18

[3] Ullal HS, von Roedern B (2007) Thin film CIGS and CdTe photovoltaic technologies: commercialization, critical issues, and applications (preprint)

[4] Green MA, Emery K, Hishikawa Y, Warta W, Dunlop ED, Levi DH, Ho-Baillie AWY (2017) Solar cell efficiency tables (version 49). Prog Photovolt Res Appl 25:3–13

[5] Fthenakis V (2009) Sustainability of photovoltaics: the case for thin-film solar cells. Renew Sustain Energy Rev 13:2746–2750

[6] Nguyen KC, Willmore WG, Tayabali AF (2013) Cadmium telluride quantum dots cause oxidative stress leading to extrinsic and intrinsic apoptosis in hepatocellular carcinoma HepG2 cells. Toxicology 306:114–123

[7] Ennaoui A, Fiechter S, Jaegermann W, Tributsch H (1986) Photoelectrochemistry of highly quantum efficient single-crystalline *n*-FeS_2 (pyrite). J Electrochem Soc 133:97–106

[8] Kilic B, Turkdogan S (2017) Fabrication of dye-sensitized solar cells using graphene sandwiched 3D-ZnO nanostructures based photoanode and Pt-free pyrite counter electrode. Mater Lett 193:195–198

[9] Ennaoui A, Fiechter S, Pettenkofer C, Alonso-Vante N, Büker K, Bronold M, Höpfner C, Tributsch H (1993) Iron disulfide for solar energy conversion. Sol Energy Mater Sol Cells 29:289–370

[10] Yu L, Lany S, Kykyneshi R, Jieratum V, Ravichandran R, Pelatt B, Altschul E, Platt HAS, Wager JF, Keszler DA et al (2011) Iron chalcogenide photovoltaic absorbers. Adv Energy Mater 1:748–753

[11] Wang H, Salveson I (2005) A review on the mineral chemistry of the non-stoichiometric iron sulphide, Fe_{1-x} S ($0 \leq x \leq 0.125$): polymorphs, phase relations and transitions, electronic and magnetic structures. Phase Transit 78:547–567

[12] Jieratum V (2012) Iron and copper chalcogenides: photovoltaic absorber candidates and $YZrF_7$: a new upconversion host. http://ir.library.oregonstate.edu/concern/graduate_thesis_or_dissertations/ms35tc980

[13] Fredrick SJ, Prieto AL (2013) Solution synthesis and reactivity of colloidal Fe2GeS4: a potential candidate for Earth abundant, nanostructured photovoltaics. J Am Chem Soc 135:18256–18259

[14] Lim D-H, Ramasamy P, Lee J-S (2016) Solution synthesis of single-crystalline Fe2GeS4 nanosheets. Mater Lett 183: 65–68

[15] Park B-I, Yu S, Hwang Y, Cho S-H, Lee J-S, Park C, Lee D-K, Lee SY (2015) Highly crystalline Fe2GeS4 nanocrystals: green synthesis and their structural and optical characterization. J Mater Chem A 3:2265–2270

[16] Nolan BM, Chan EK, Zhang X, Muthuswamy E, van Benthem K, Kauzlarich SM (2016) Sacrificial silver nanoparticles: reducing GeI2 to form hollow germanium nanoparticles by electroless deposition. ACS Nano 10:5391–5397

[17] Xin X, He M, Han W, Jung J, Lin Z (2011) Low-cost copper zinc tin sulfide counter electrodes for high-efficiency dye-sensitized solar cells. Angew Chem Int Ed Engl 50:11739–11742

[18] Tong Z, Su Z, Liu F, Jiang L, Lai Y, Li J, Liu Y (2014) In situ prepared Cu_2ZnSnS_4 ultrathin film counter electrode in dye-sensitized solar cells. Mater Lett 121:241–243

[19] Chiang HC, Wang MH, Ueng CH (1993) Synthesis and structure of diaquabis(glycolato-O, O'')germanium(IV). Acta Crystallogr Sect C 49:244–246

[20] Kalyanasundaram K, Grätzel M (2009) Efficient dye-sensitized solar cells for direct conversion of sunlight to electricity. Mater Matters 4:88–90